Supporting information

Terbium alginate encapsulated $CsPbI_3$@Pb-MOF: A ratiometric fluorescent bead for detection and adsorption of Fe^{3+}

Yangwen Hou[a], Hua Feng[b], Jingting He[a], Fanfei Meng[b], Jing Sun[b], Xiao Li[b], Xinlong Wang[c], Zhongmin Su[b,d,*], Chunyi Sun[c,*]

[a]School of Materials Science and Engineering, Changchun University of Science and Technology, Changchun 130022 Jilin, China

[b]Jilin Provincial Science and Technology Innovation Center of Optical Materials and Chemistry, School of Chemistry and Environmental Engineering, Changchun University of Science and Technology Changchun, Changchun, 130022 Jilin, China

[c]Key Laboratory of Polyoxometalate Science of Ministry of Education, Northeast Normal University, Changchun, 130024 Jilin, China

[d]State Key Laboratory of Supramolecular Structure and Materials, Institute of Theoretical Chemistry, College of Chemistry, Jilin University, Changchun, 130021 Jilin, China

* Corresponding author.

E-mail addresses: zmsu@nenu.edu.cn (Z. Su), suncy009@nenu.edu.cn (C. Sun).

1.Experimental section

1.1 FL detection of Fe^{3+}

To measure sensitivity, a mixture of 50 mg $CsPbI_3$@Pb-MOF@Tb-AG and varying concentrations of Fe^{3+} (ranging from 0 to 90 μM) was prepared. Subsequently, fluorescence spectra were recorded using an excitation wavelength of 448 nm. To determine probe selectivity, various Ag^{+}, Na^{+}, K^{+}, Cd^{+}, Ca^{2+}, Cu^{2+}, Ni^{2+}, Co^{2+}, Mn^{2+}, Zn^{2+}, Mg^{2+}, Ba^{2+}, Pb^{2+}, Cd^{2+}, Al^{3+}, In^{3+}, Cr^{3+}, Br^{-}, Cl^{-}, SO_4^{2-} and NO_3^{-}ions including were prepared at a concentration of 50 μM. The solutions above and 50 μM of Fe^{3+} solution were added to the mixture individually, and the changes in fluorescence were monitored.

1.2 Adsorption experiments

Firstly, the dry sample (10 mg) is mixed with a Fe^{3+} solution (20 mL, 400 mg/L) and magnetically stirred for 24 hours. Subsequently, the supernatant was collected for the ICP test.

1.3 Characterization

X-ray diffraction analysis utilized a Rigaku Ultima IV diffractometer at 40 kV and 30 mA, employing Cu Kα radiation (λ = 1.5406 Å). We conducted scans from 5° to 60° 2θ, at 0.02° increments and 1-second dwell time per step. Photoluminescence spectra were acquired using a F98 spectrofluorometer, under 365 nm excitation and 5 nm slit widths, across a 500-700 nm wavelength range at ambient temperature. Energydispersive X-ray spectroscopy (EDS) and scanning electron microscopy (SEM) images were obtained with a Hitachi TM-1000 tabletop SEM, setting the electron beam to 15 keV, a 35° take-off angle, a 10 mm working distance, and 60 seconds acquisition time. Transmission electron microscopy (TEM) and high-resolution TEM (HRTEM) analyses employed a JEOL JEM-2010 microscope at 200 kV, achieving a 0.19 nm spatial resolution, using carbon-coated copper grids and a Gatan Orius CCD camera for image capture and DigitalMicrograph software for analysis. X-ray photoelectron spectroscopy (XPS) was performed on an Escalab 250, using monochromatic Al Kα radiation (1486.7 eV), with a 45° take-off angle, electron flood gun for charge compensation, and C 1s calibration at 284.8 eV. High-resolution and survey scans utilized 20 eV and 160 eV pass energies, respectively, with three scans and a 0.1 eV resolution, employing Lorentzian-Gaussian mix fitting (20% Lorentzian). UV-Vis diffuse reflectance spectra were characterized on a TU-1900 spectrophotometer, spanning 200-800 nm, using barium sulfate as a standard. Fluorescence lifetimes were measured with an Edinburgh Instruments FLS980 spectrofluorometer, using a 375 nm, 100 ps pulsed diode laser, covering a 400-800 nm detection range with 5 ps resolution, and setting data collection to 5 minutes per sample.

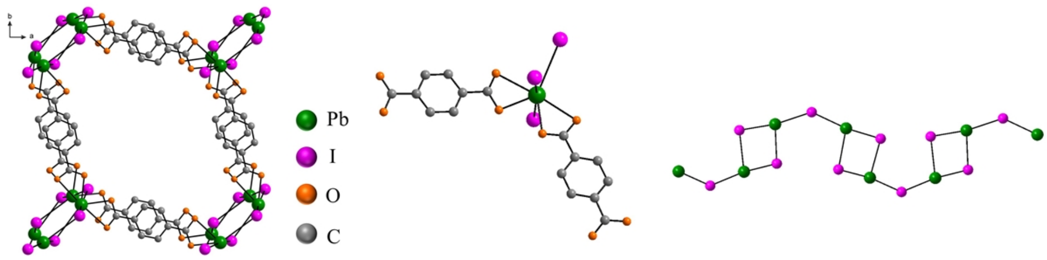

Fig.S1. Crystallographic view of PbI-MOF.

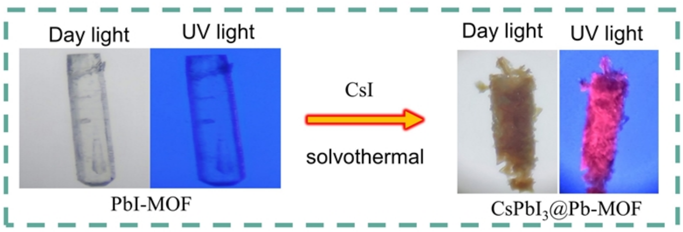

Fig.S2. Photographs of $CsPbI_3$@Pb-MOF under daylight and UV light (365 nm).

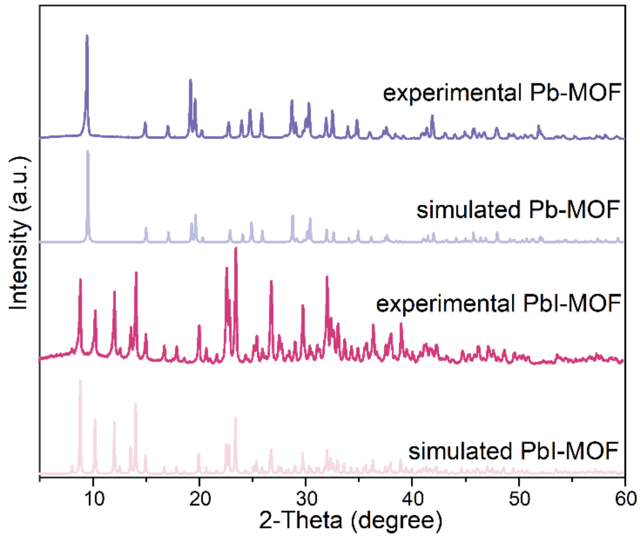

Fig.S3. PXRD pattern of PbI-MOF and Pb-MOF.

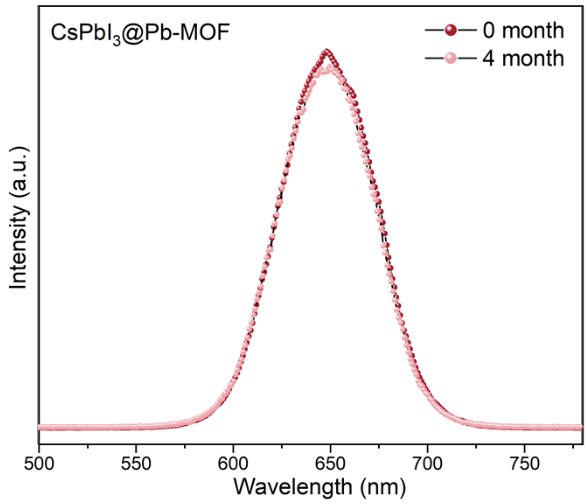

Fig.S4. PL spectra of $CsPbI_3$@Pb-MOF in water at different times.

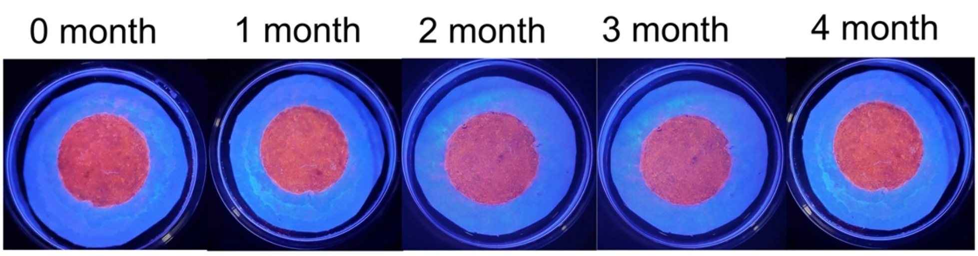

Fig.S5. The image displays $CsPbI_3$@Pb-MOF samples in water at different times.

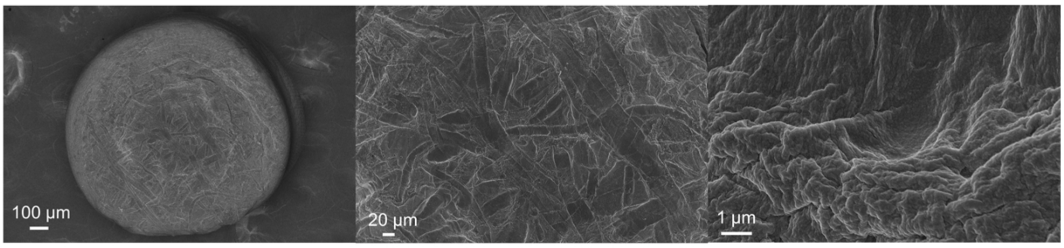

Fig. S6. SEM of the pure Tb-AG.

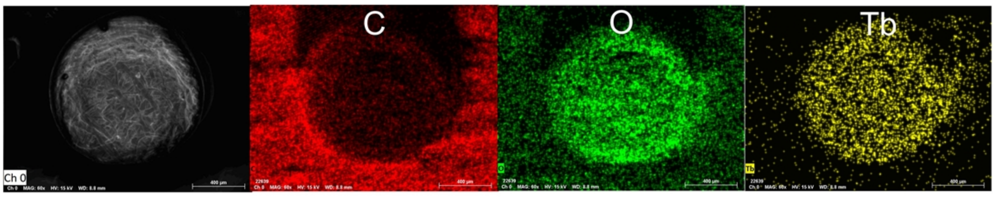

Fig. S7. EDS element mapping of the pure Tb-AG.

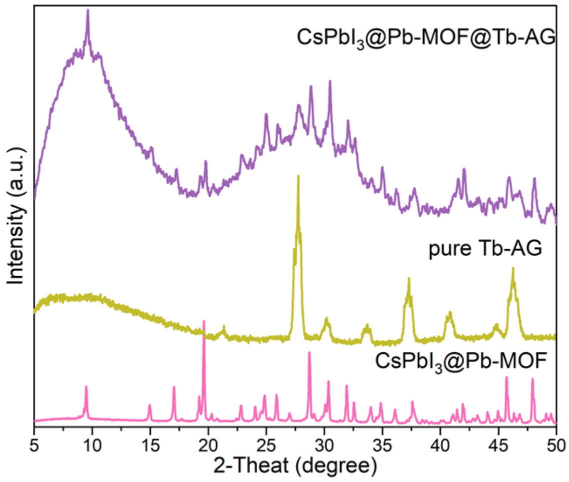

Fig.S8. PXRD pattern of samples.

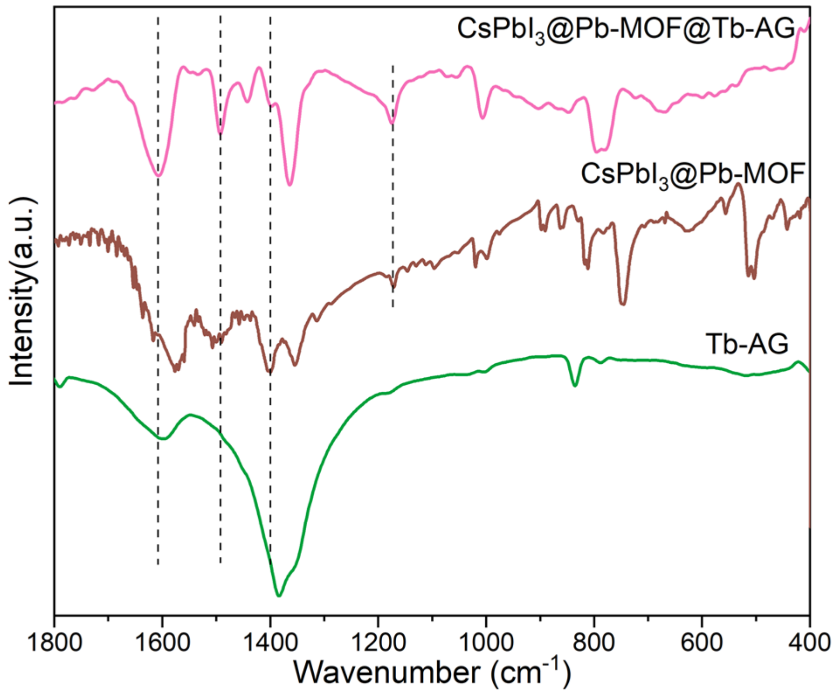

Fig.S9. FTIR of samples.

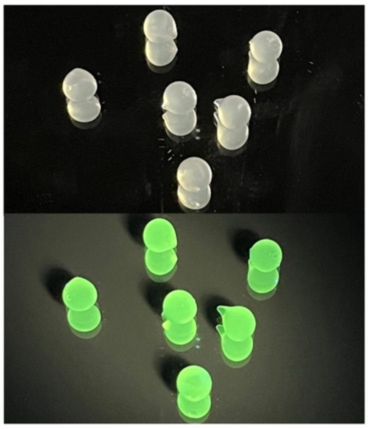

Fig.S10. The image displays Tb-AG samples under two conditions: daylight and UV light irradiation.

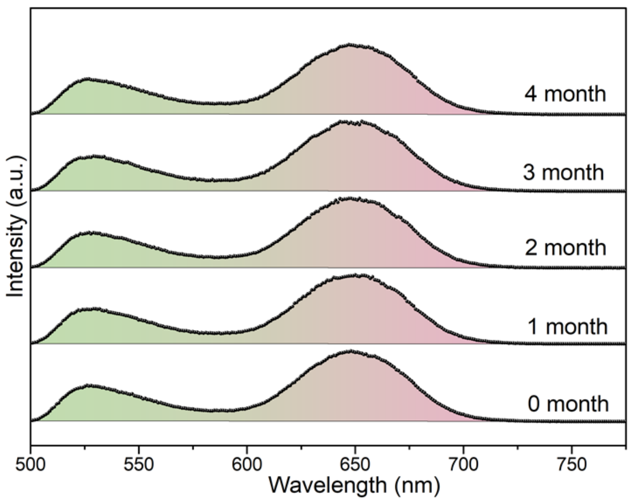

Fig.S11. PL spectra of $CsPbI_3$@Pb-MOF@Tb-AG in water at different times.

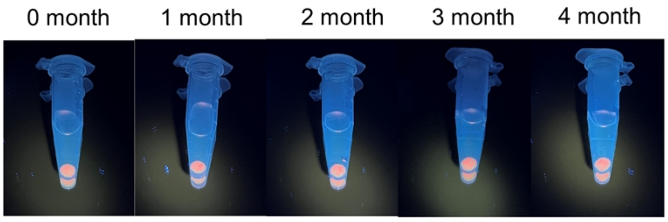

Fig.S12. The image displays $CsPbI_3$@Pb-MOF@Tb-AG samples in water at different times.

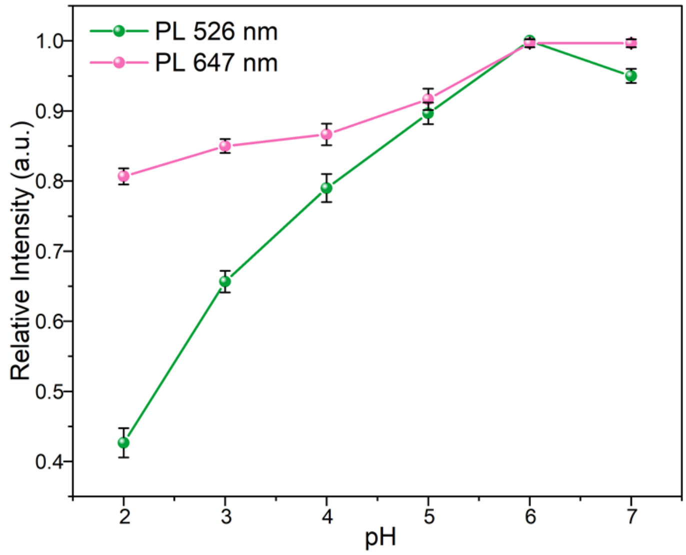

Fig. S13. The quenching efficiency of $CsPbI_3$@Pb-MOF@Tb-AG for Fe^{3+} (10μM) under the different pH conditions.

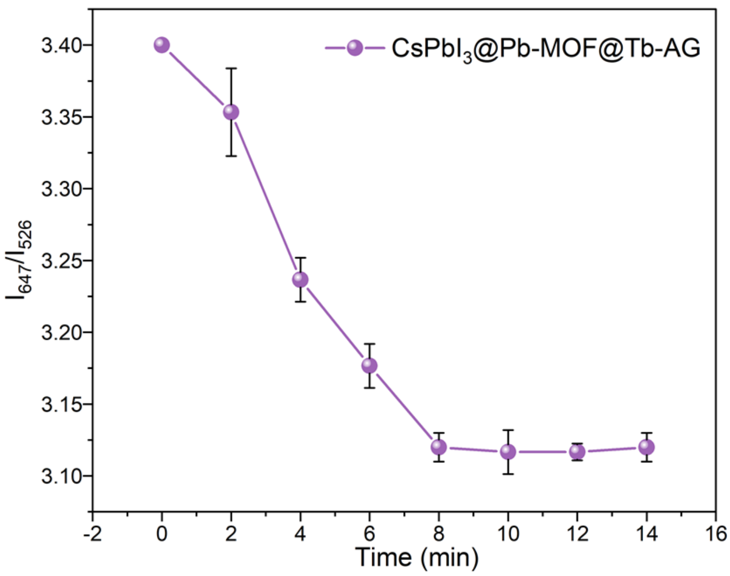

Fig. S14. Time-dependent fluorescence intensity of $CsPbI_3$@Pb-MOF@Tb-AG upon addition of Fe^{3+} (10 μM, pH=6).

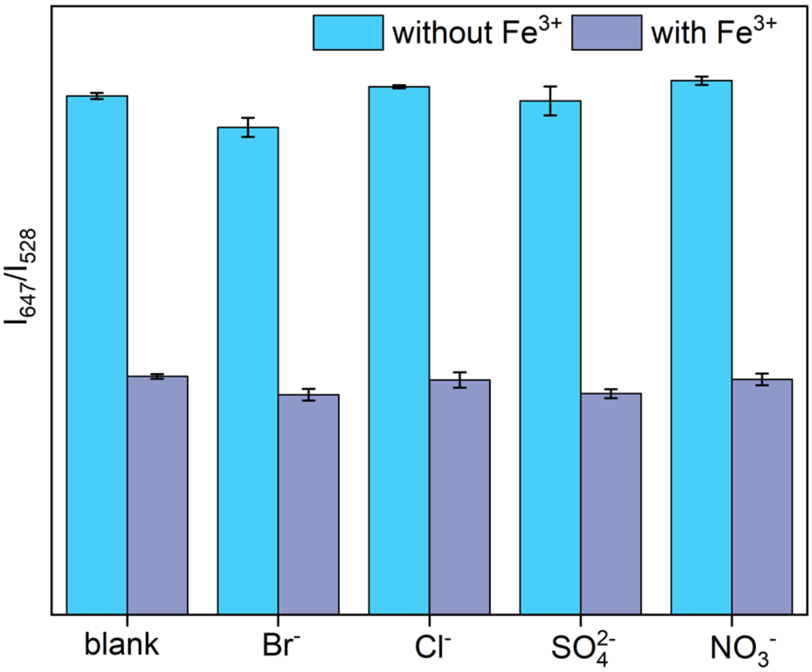

Fig.S15. Analysis of the impact of various anion on the relative fluorescence intensity (I_{647}/I_{528}) of $CsPbI_3$@Pb-MOF@Tb-AG, both with and without the presence of Fe^{3+}.

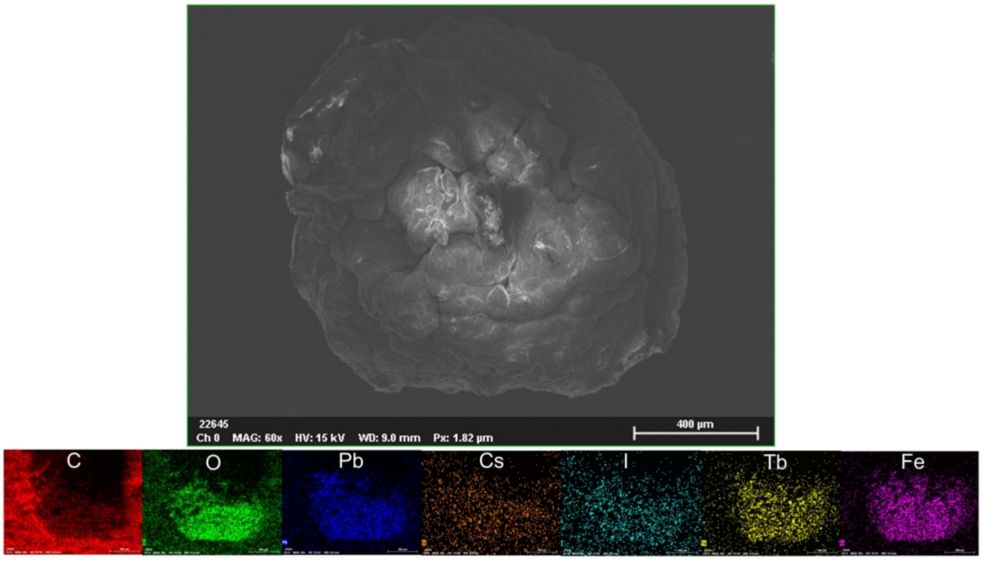

Fig.S16. SEM and EDS of $CsPbI_3$@Pb-MOF@Tb-AG+Fe^{3+}.

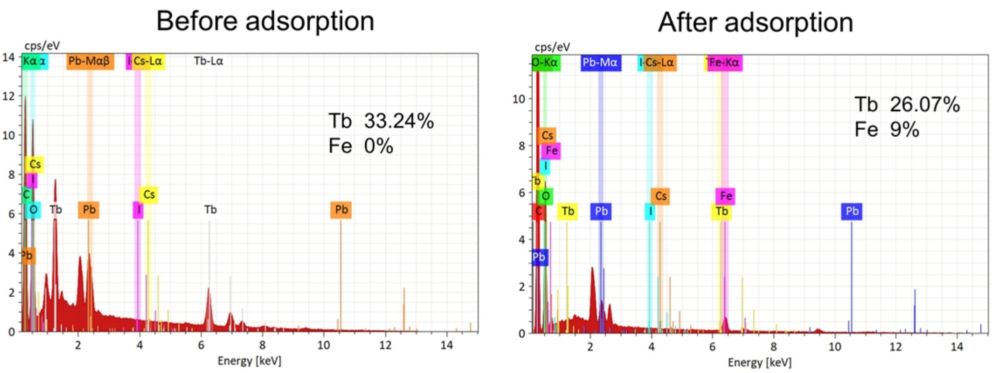

Fig.S17. EDS of $CsPbI_3$@Pb-MOF@Tb-AG before and after adsorbing Fe^{3+}.

Table S1. Time-resolved PL decay parameters of different samples under 448 nm excitation. The two-exponential decay curves were fitted using a non-linear least-squares method with a two-component decay law. The average lifetime (τ_{av}) was then determined using the equation:

$$\tau = \sum_{i=1}^{i=n} A_i \tau_i^2 / \sum_{i=1}^{i=n} A_i \tau_i$$

Sample	**τ_1(ns)**	**τ_2(ns)**	**X^2**	**τ_{av}(ns)**
$CsPbI_3$@PbI-MOF	15.34 (10.58%)	37.50 (89.42%)	1.103	35.15
$CsPbI_3$@PbI-MOF@Tb-AG	16.20 (17.26%)	47.48 (82.74%)	1.125	42.09

Table S2. Comparison of the detection and adsorption of Fe^{3+} ions using different Materials.

Sensing materials	Linear range (μM)	LOD (μM)	Adsorption capacity (mg/g)	Ref.
Carbon dot	1-100	0.32	-	1
N-doped Carbon dot	1-250	0.52	-	2
Nitrogen-doped carbon dots	2-25	0.9	-	3
$CsPbBr_3$@PSAA	5-150	2.2	-	4
SiO_2@$CsPbBr_3$@SiO_2	10-70	3	-	5
Bone gelatin $CsSnCl_3$	0-2000	8	-	6
Eu^{3+}@Uio-66-CA	0-250	18.1	-	7
TiO_2-banana cluster	-	-	150	8
SiO_2@Nap	0-125	1.32	79	9
PNIPAAm-CD hydorgel	1-1000	0.27	280.25	10
CsPbI3@Pb-MOF@Tb-AG	0-90	0.44	325.4	This work

Table S3. Time-resolved PL decay parameters of different samples under 448 nm excitation. The two-exponential decay curves were fitted using a non-linear least-squares method with a two-component decay law. The average lifetime (τ_{av}) was then determined using the equation:

$$\tau = \sum_{i=1}^{i=n} A_i \tau_i^2 / \sum_{i=1}^{i=n} A_i \tau_i$$

Sample	**τ_1(ns)**	**τ_2(ns)**	**X^2**	**τ_{av}(ns)**
$CsPbI_3$@PbI-MOF@Tb-AG	16.20	47.48	1.125	42.09
	(17.26%)	(82.74%)		
$CsPbI_3$@PbI-MOF@Tb-AG+20μM	7.57	37.97		
	(3.41%)	(96.59%)	1.135	39.25
$CsPbI_3$@PbI-MOF@Tb-AG+40μM	7.17	35.19		
	(10.38%)	(89.62%)	1.194	32.28

References

[1] J. Shen, S. Shang, X. Chen, D. Wang, Y. Cai, *Mater. Sci. Eng. C.*, 2017, **76**, 856–864.

[2] Y. Song, C. Zhu, J. Song, H. Li, D. Du, Y. Lin, *ACS Appl. Mater. Inter.*, 2017, **9**, 7399–7405.

[3] R. Atchudan, T.N.J.I. Edison, K.R. Aseer, S. Perumal, N. Karthik, Y.R. Lee, *Biosens. Bioelectron.*, 2018, **99**, 303–311.

[4] M. Chen, J. An, Y. Hu, R. Chen, Y. Lyu, N. Hu, M. Luo, M. Yuan, Y. Liu, *Sensor Actuat B-Chem.*, 2020, **325**, 128809.

[5] X.-H. Tan, G.-B. Huang, Z.-X. Cai, F.-M. Li, Y.-M. Zhou, M.-S. Zhang, *J Anal Test.*, 2021, **5**, 40–50.

[6] D. Gao, Y. Zhang, B. Lyu, X. Guo, Y. Hou, J. Ma, B. Yu, S. Chen, *Inorg. Chem.*, 2022, **61**, 6547–6554.

[7] Y. Fan, X. Sun, W. Zhang, J. Liu, *Colloids Surf. A Physicochem. Eng. Asp.*, 2023, **669**, 131513.

[8] S. Chatterjee, H. Gohil, A.R. Paital, *ChemistrySelect.*, 2017, **2**, 5348–5359.

[9] C. Wang, T. Hu, Z. Wen, J. Zhou, X. Wang, Q. Wu, C. Wang, *J. Colloid. Interf. Sci.*, 2018, **521**, 33–41.

[10] D. Zhang, X. Tian, H. Li, Y. Zhao, L. Chen, *Colloids Surf. A Physicochem. Eng. Asp.*, 2021, **608**, 125563.